WORLD CONFERENCE ON TIMBER ENGINEERING 2025
BRISBANE, AUSTRALIA
Advancing Timber for the Future Built Environment

COMPRESSIVE BEHAVIOR OF TIMBER AT DIFFERENT ORIENTATIONS TO THE GRAIN

Marina Totsuka[1]*, Rina Okada[2], Kenji Aoki[3]

ABSTRACT: Timber members are often compressed off-axis in timber connections. Off-axis compressive strength and stiffness, including a spreading effect, are essential to design timber structures. In this paper, compression and partial compression tests at different orientations were conducted to clear the influence of loading angles, spreading effects, and damage zones. Young's modulus and strength of the compression and partial compression tests depended on the loading angle for the longitudinal direction. Deformations and failure behavior were also strongly influenced by the loading angle. Kink band failure often occurred in the specimens at the loading angle of 0 degrees, shear failure often occurred at 15 and 30 degrees, and compressive failure perpendicular to the grain often occurred at 30, 45, 60, and 90 degrees. The spreading effect increased with increasing the loading angles in the Young's modulus and strength. We proposed an evaluation method of the off-axis compressive stiffness and strength, including the spreading and damage zone effects, using Hankinson's equation.

KEYWORDS: Wood, Off-axis compressive behavior, Young's modulus, Hankinson's equation, spreading effect

1 – INTRODUCTION AND BACKGROUND

Wood is orthotropic in three primary directions: longitudinal (L), radial (R), and tangential (T). In practical applications of timber as a construction material, compressive loads frequently act in various orientations relative to the grain, extending beyond just these three main directions, as shown in Fig. 1.

Several studies conducted on off-axis compression, focusing on Young's modulus and strength using small specimens, e.g. [1]–[4]. Young's modulus and strength were evaluated in off-axis compression using Hankinson's equation [5], [6]. However, these investigations have neglected to consider the behavior around the loading plate.

Under compression parallel to the grain, it has been observed that the largest strains are allocated near the loading plates[7], which are collectively referred to as “damage zones” (Fig. 2). A zone in between them is referred to as a “middle zone.” Xavier et al.[2] and Totsuka et al.[8], [9] Investigated the behavior of the damage zones (e.g., the length and modulus of elasticity of the damage zones).

Partial compressions are more complex because of a spreading [10] and the damage zone effects [11] and often occur in the timber connections. However, the

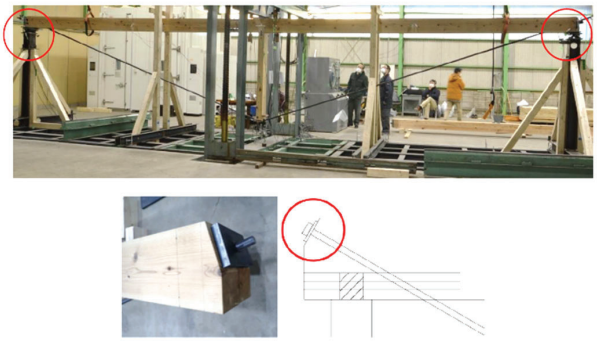

Figure 1. Example of timber connection.

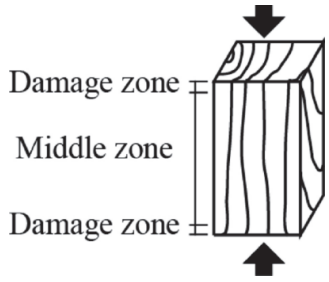

Figure 2. Explanation of damage and middle zones

[1]* Corresponding author, Marina Totsuka, Graduate School of Engineering, Chiba University, Chiba, Japan, 263-8522, ORCID 0000-0001-8548-4996
[2] Okada Rina, Former The Univ. of Tokyo.
[3] Kenji Aoki, Graduate School of Agricultural and Life Sciences, The Univ. of Tokyo, Tokyo, Japan,

https://doi.org/10.52202/080513-0673

number of studies of partial off-axis compression is limited.

This paper investigates the off-axis compression and partial compression behavior of glulam. A method for evaluating the compressive strength and stiffness is proposed, which incorporates the effects of spreading and damage zones using Hankinson's equation.

2 – PROJECT DESCRIPTION

Off-axis compression tests were conducted. Table 1 shows an overview of the test series. Fig.3 shows load cases with and without a side margin. Specimens were made from homogeneous glulam of Japanese cedar (*Cryptomeria japonica*, average mass density was 395 kg/m^3, average moisture content was 14.0 %) of quality E65-F255 and Japanese larch (*Larix leptolepis*, average mass density was 492 kg/m^3, average moisture content was 15.7 %) of quality E95-F315 according to JAS (Japanese Agricultural Standards[12]). Dimensions of the specimens were length 30-165 mm × width 30 mm × height 90 mm. A loaded area was 30 mm × 30 mm. A total of 131 specimens were prepared by manufacturing 2-7 samples per series. Test variables were wood species (Japanese cedar or Japanese larch), the side margin (with or without), and loading angles (0, 15, 30, 45,60, or 90 degrees). For instance, the loading angle of 0 degrees indicates the compression parallel to the grain.

3 – EXPERIMENTAL SETUP

A test method was based on ASTM[13]. The compression tests were carried out on a 100 kN universal testing machine with an in-line load cell and two displacement transducers to measure a vertical displacement of the total height of the specimens, see Fig.4. The 2D deformations and local strains in a surface were also measured by a DIC system by a digital camera. Pictures were captured at a frequency of 0.2 Hz during the test. The images were processed with a DIC software (GOM correlate, GOM, Braunschweig, Germany). A speckle pattern, which consisted of black dots on a white surface, was painted on the side face of these specimens. The specimens were subjected to a monotonical load-controlled a 0.27 mm/min deformation rate through a steel plate until failure or the displacement exceeded 5 mm.

4 – RESULTS

Stress-strain curves are shown in Fig.5. Stress σ was determined by:

Table 1: Overview of specimens

Series	Timber	side margin	Loading angle	#
S-A-0	Homogeneous glulam of Japanese cedar	without	0°	6
S-A-15		without	15°	7
S-A-30		without	30°	7
S-A-45		without	45°	7
S-A-60		without	60°	7
S-A-90		without	90°	6
S-P-15		with	15°	6
S-P-30		with	30°	6
S-P-45		with	45°	6
S-P-60		with	60°	6
S-P-90		with	90°	6
K-A-0	Homogeneous glulam of Japanese larch	without	0°	3
K-A-15		without	15°	3
K-A-30		without	30°	3
K-A-45		without	45°	3
K-A-60		without	60°	3
K-A-90		without	90°	2
K-P-15		with	15°	3
K-P-30		with	30°	3
K-P-45		with	45°	3
K-P-60		with	60°	3
K-P-90		with	90°	3

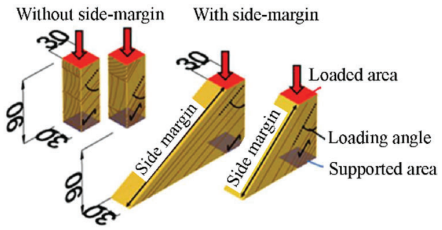

Figure 3. Load cases with or without side margin.

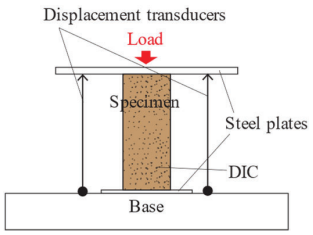

Figure 4. Loading set-up and measurements

$$\sigma = \frac{P}{A} \quad (1)$$

Where P is the load measured by the load cell, A is the loaded area. Strain ε was determined by:

$$\varepsilon = \frac{\Delta l}{H} \quad (2)$$

Where l is the average displacement measured by the two displacement transducers, and H is the original specimen height.

In the Japanese cedar specimens, kink band failure often occurred in the specimens at the loading angle of 0

https://doi.org/10.52202/080513-0673

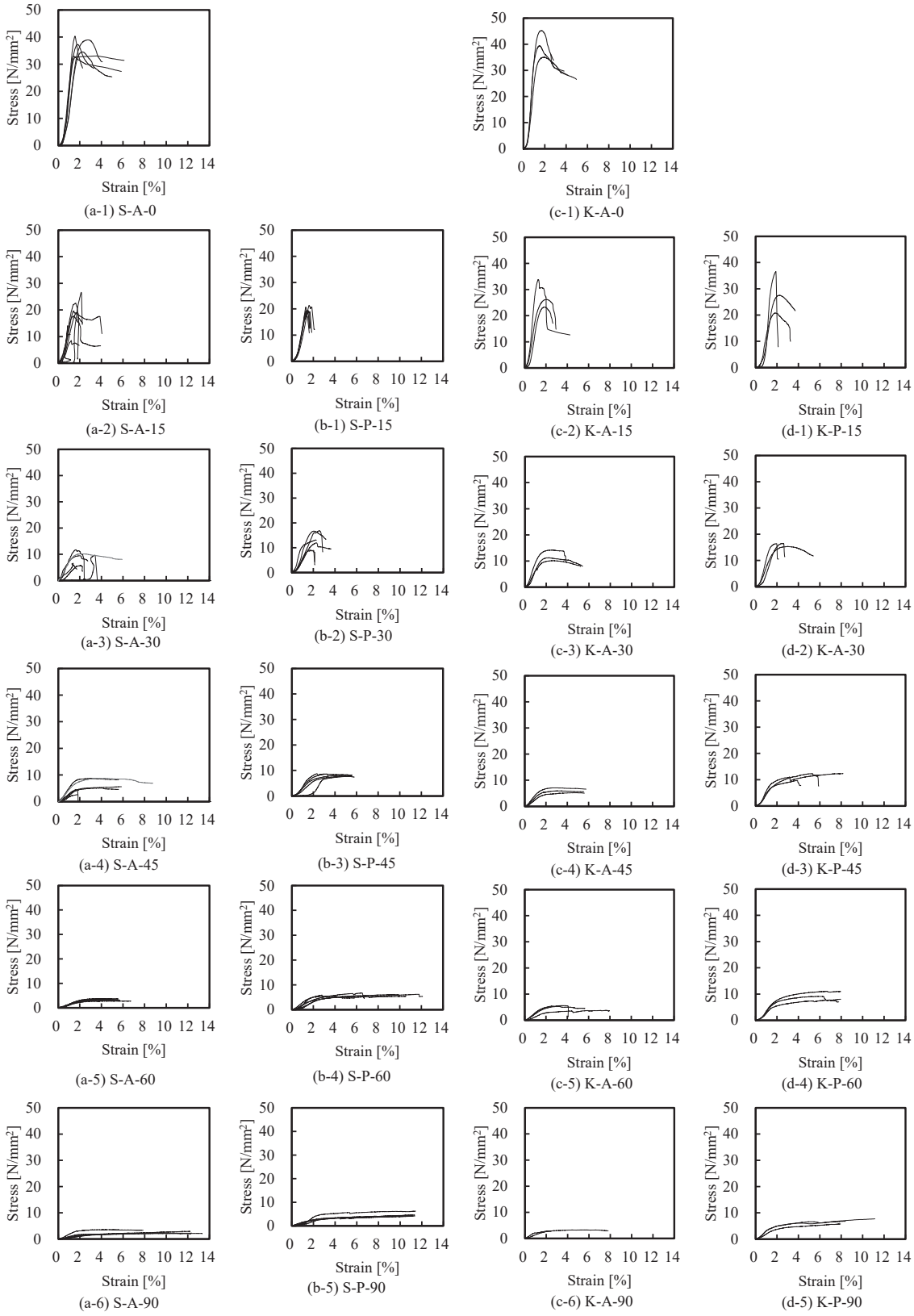

Figure 5. Stress-strain curves

https://doi.org/10.52202/080513-0673

degrees, as shown in Fig.6(a), and the stress-strain curves exhibited brittle behavior due to plastic buckling, as shown in Fig.5(a-1). Shear failure often occurred at 15 and 30 degrees, as shown in Fig.6(b), and the stress-strain curves exhibited brittle behavior, as shown in Fig.5(a-2)(a-3)(b-1)(b-2), regardless of with and without the side margin. Compressive failure perpendicular to the grain often occurred at 45, 60, and 90 degrees, as shown in Fig.6(c) , and the stress-strain curves exhibited ductile behavior, as shown in Fig.5(a-4)(a-5)(a-6)(b-3)(b-4)(b-5), regardless of with and without the side margin.

In Japanese larch specimens, a kink band failure often occurred in the specimens at the loading angle of 0 degrees, and the stress-strain curves exhibited brittle behavior due to plastic buckling, as shown in Fig.5(c-1). Shear failure often occurred at 15 degrees, and the stress-strain curves exhibited brittle behavior, as shown in Fig.5(c-2)(d-1), regardless of with and without the side margin. Compressive failure perpendicular to the grain often occurred at 30, 45, 60, and 90 degrees, and the stress-strain curves exhibited ductile behavior, as shown in Fig.5(c-3)(c-4)(c-5)(c-6)(d-2)(d-3)(d-4)(d-5), regardless of with and without the side margin.

5 – DISCUSSION

A proportional limit stress σ_p was determined as follows: A point at 20% of the maximum stress σ_{max} was taken as a starting point for calculating a regression line. The stress at a point i, where a ratio of a slope of the regression line for 30 points from the point i to the slope of the regression line for 30 points from a point $i-29$ first becomes 1.2 times, was defined as the proportional limit stress.

The Young's modulus E was determined by:

$$E = \begin{cases} \dfrac{0.4\sigma_{\max} - 0.2\sigma_{\max}}{\varepsilon_{0.4\sigma_{\max}} - \varepsilon_{0.2\sigma_{\max}}} & \text{if there is } \sigma_{\max}, \\ \dfrac{0.4\sigma_{5\mathrm{mm}} - 0.2\sigma_{5\mathrm{mm}}}{\varepsilon_{0.4\sigma_{5\mathrm{mm}}} - \varepsilon_{0.2\sigma_{5\mathrm{mm}}}} & \text{if there is no } \sigma_{\max} \end{cases} \quad (4)$$

Where $\varepsilon_{0.4\sigma max}$ or $\varepsilon_{0.2\sigma max}$ is the strain at the 0.4 or 0.2 σ_{max}, σ_{5mm} is the stress at 5mm, $\varepsilon_{0.4\sigma 5mm}$ or $\varepsilon_{0.4\sigma 5mm}$ is the strain at the 0.4 or 0.2 σ_{5mm}.

5.1 RELATIONSHIPS BETWEEN PROPORTIONAL LIMIT STRESS OR YOUNG'S MODULUS AND LOADING ANGLES

Fig. 7 shows relationships between the proportional limit stress or Young's modulus and loading angles with or without the side margin. The proportional limit stress and

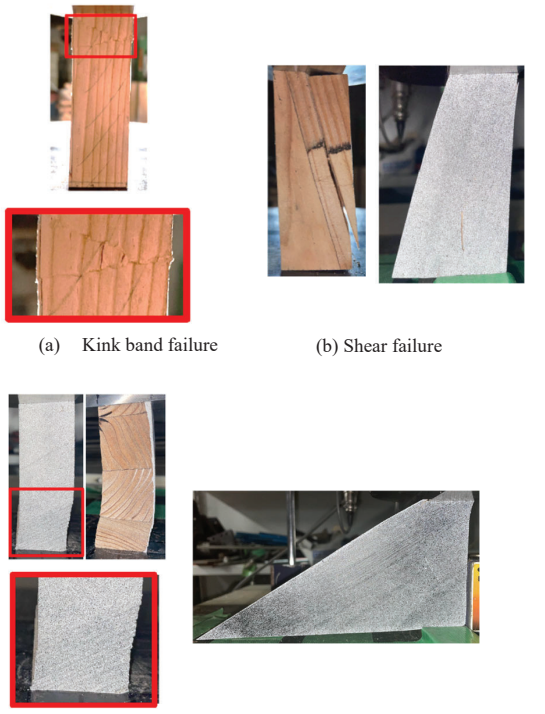

Figure 6. Failure modes of cedar specimens with or without side margin

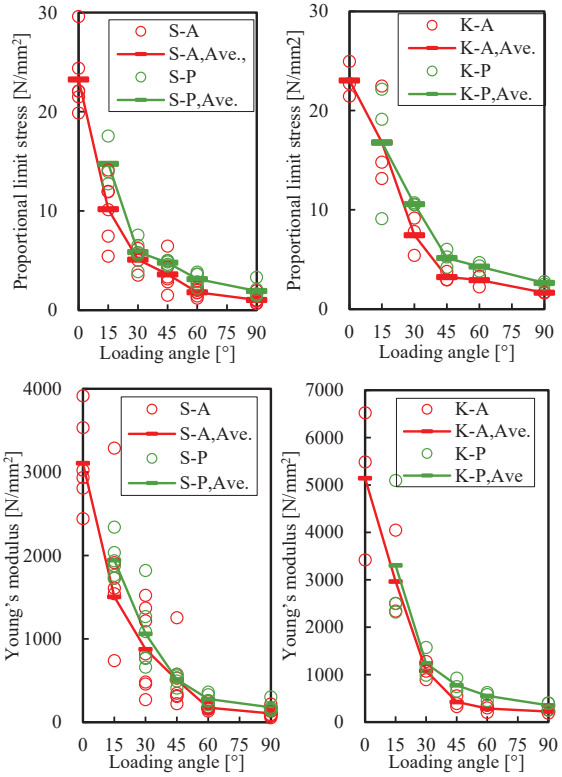

Figure 7. the relationship between the proportional limit stress or Young's modulus and loading angles with or without the side margin

https://doi.org/10.52202/080513-0673

Young's modulus almost increased with decreasing the loading angles. The proportional limit stress and Young's modulus of the specimens with the side margin are larger than those of the specimens without the side margin.

5.2 SPREADING EFFECT

A t-test was conducted to examine a significant difference between the proportional limit stress or Young's modulus of the specimens with and without the side margin. Results are shown in Table 2. For the proportional limit stress, the P-values were small for most loading angles. For the Young's modulus, the limited effects were observed at loading angles of 15 degrees (P value = 0.35), 30 degrees (P value = 0.24), and 45 degrees (P value = 0.48), but significant differences were observed at 60 degrees (P value = 0.002) and 90 degrees (P value = 0.033) in the Japanese cedar specimens and at loading angles of 15 degrees (P value = 0.38), 30 degrees (P value = 0.25), but significant differences were observed at 45 degrees (P value = 0.014), 60 degrees (P value = 0.008) and 90 degrees (P value = 0.066) in the Japanese larch specimens. Therefore, it is considered that the spreading effect is present in most loading angles in the proportional limit stress and is present at loading angles of 45 degrees or more in the Young's modulus.

Spreading effects of the proportional limit stress k_σ (5) and the Young's modulus k_E (6) are defined as ratios of the specimens without the side margin to those with the side margin.

$$k_\sigma = \frac{\sigma_{p,P}}{\sigma_{p,A}} \tag{5}$$

$$k_E = \frac{E_P}{E_A} \tag{6}$$

Where $\sigma_{p,P}$, $\sigma_{p,A}$ are the proportional limit stress of the specimen with($\sigma_{p,P}$) or without($\sigma_{p,A}$) the side margin, E_P, E_A is the Young's modulus of the specimen with(E_P) or without(E_A) the side margin. The relationships between the spreading effects and the loading angles are shown in Fig.8. The k_σ was 1.0-1.9, and the k_E was 1.0-1.9. The k_σ and k_E increased as loading angles increased. There is a smaller effect at a smaller loading angle because there is no spreading effect under compression parallel to the grain (loading angle 0 degrees), and there is a larger effect at a larger loading angle the spreading effect because the spreading effect is confirmed under compression perpendicular to the grain (loading angle 90 degrees).

5.3 DAMAGE ZONES EFFECT

Table 2: Results of t-test between the Young's modulus of the specimens with and without the side margin

	Japanese cedar specimen				
Loading angle	15°	30°	45°	60°	90°
P-value for σ_p	0.033	0.176	0.063	0.001	0.015
P-value for E	0.349	0.244	0.484	0.002	0.033
	Japanese larch specimen				
P-value for σ_p	0.499	0.052	0.025	0.017	0.043
P-value for E	0.383	0.253	0.014	0.008	0.066

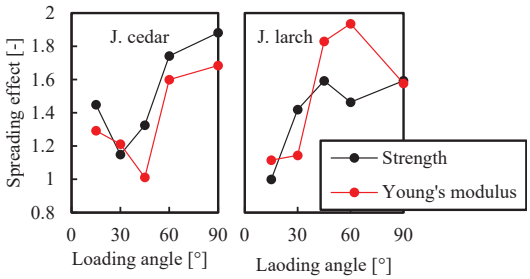

Figure 8. Spreading effect and loading angle

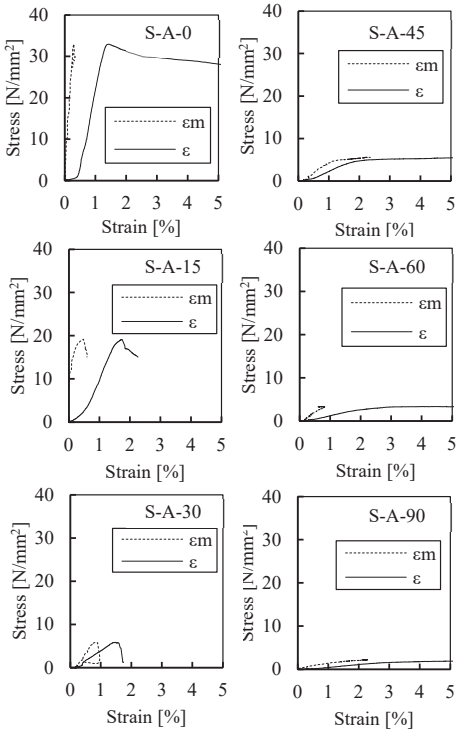

Figure 9. Stress-strain curves of the full height ε and the middle zone, which is the zone in between the damage zones

The damage zones were observed in all specimens. The stress-strain curves of the full height ε (2) and a middle zone ε_m, which is the zone in between the damage zones, in the S-A specimens are shown in Fig.9. The strain of the middle zone ε_m was the mean value of a red area in Fig.10 and measured by the DIC. The strain of the ε was larger than that of the ε_m in all specimens.

https://doi.org/10.52202/080513-0673

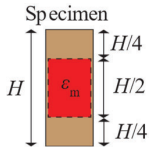

Figure 10. Explanation of strain of middle zone

Table 3: Young's modulus of full height (E) and middle zone (Em)

Series	S-A-0	S-A-15	S-A-30	S-A-45	S-A-60	S-A-90
The Young's modulus E [N/mm^2]	3376	1609	485	338	167	67
The Young's modulus E_m [N/mm2]	12291	90244	870	795	389	151

To investigate the relationship between the loading angles and the effect of the damage zone on the Young's modulus of the full specimen, a comparison of the Young's modulus of the full height (E) and the Young's modulus of the middle zone (E_m) is shown in Table 3. The method for calculating the Young's modulus is the same as in (4). The relationship between the loading angles and the ratio E/E_m is shown in Fig.11. The smaller ratio E/E_m indicates a greater effect on the damage zone. The effect of the damage zone was not large at the loading angles of 30 to 90 degrees (E/E_m = 0.43 to 0.56) compared to 0 and 15 degrees (E/E_m = 0.27 and 0.02). Therefore, it is considered that the damage zone is present in all specimens with different loading angles, and the influence of the damage zone is particularly pronounced at loading angles of 0 and 15 degrees.

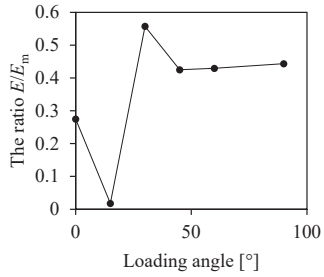

Figure 11. relationship between loading angles and ratio E/E_m

5.3 APPLICATION OF HANKINSON'S EQUATION

Hankinson's equations[6] for the proportional limit stress and Young's modulus were in:

$$\sigma_{p,\theta} = \frac{\sigma_{p,0}\sigma_{p,90}}{\sigma_{p,0}\sin\theta^n + \sigma_{p,90}\cos\theta^n} \quad (7)$$

$$E_\theta = \frac{E_0 E_{90}}{E_0 \sin\theta^n + E_{90}\cos\theta^n} \quad (8)$$

Where $\sigma_{p,0}$, $\sigma_{p,90}$ is the proportional limit stress at the loading angle 0 or 90 degrees, θ is the loading angle, and E_0, E_{90} is the Young's modulus at the loading angle 0 or 90 degrees. The exponent n, determined by a load type, can take values between 1.5 and 2 and is 2 when calculating the Young's modulus. The experimental results and Hankinson's equations are shown in Figure 12. For all specifications, Hankinson's equation with n=2 matches or slightly underestimates the average experimental values.

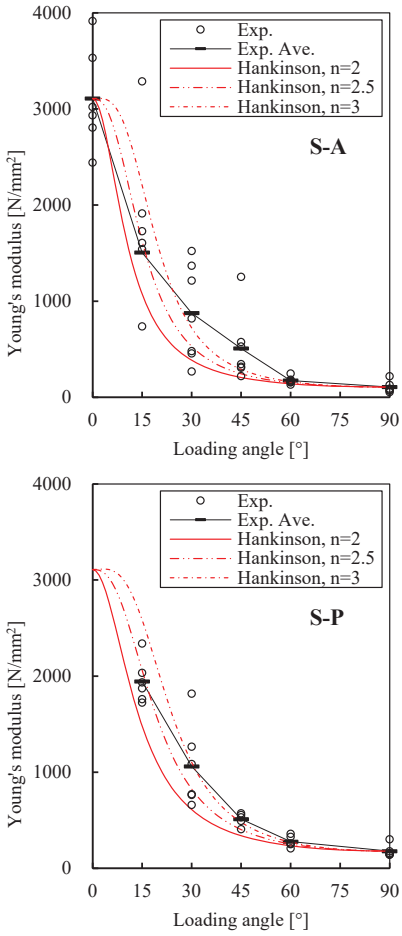

Figure 12 Experimental results and Hankinson's equations

https://doi.org/10.52202/080513-0673

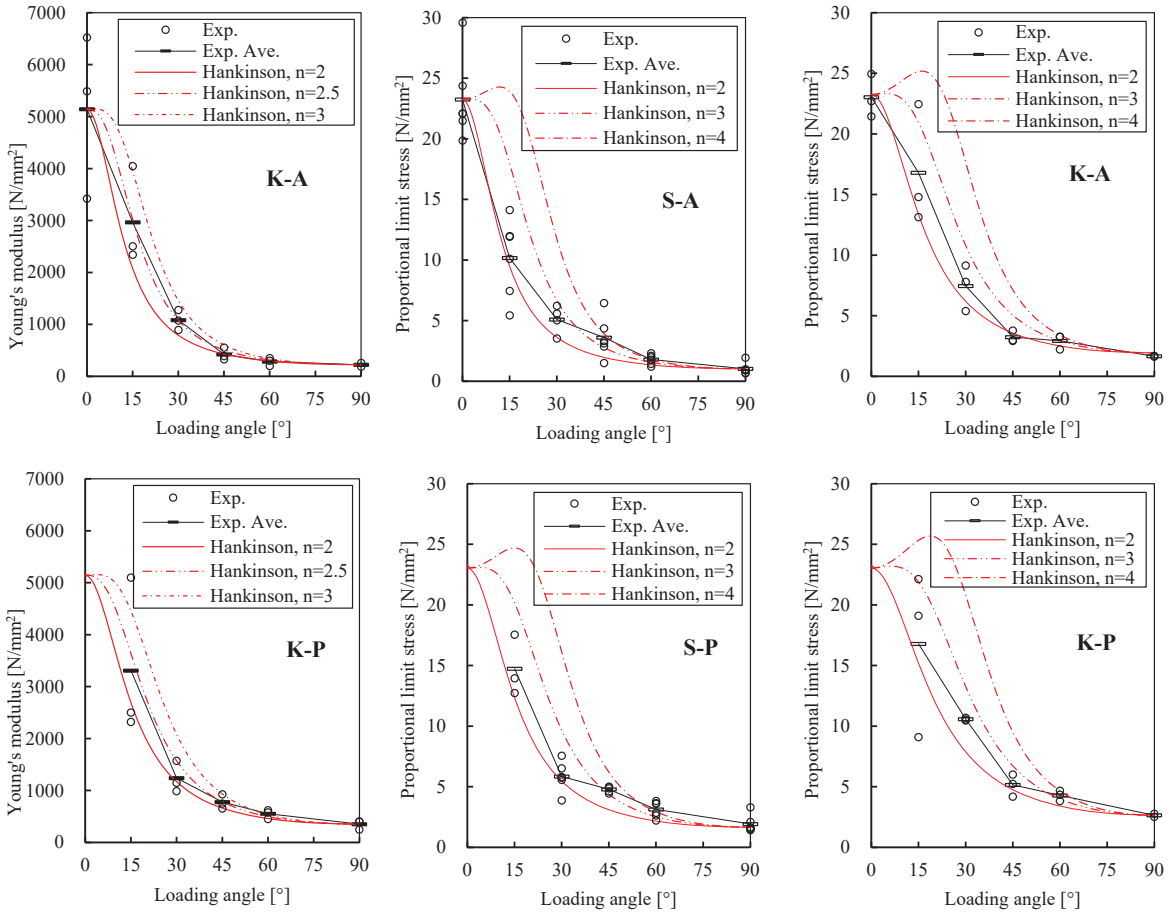

Figure 12 *Experimental results and Hankinson's equations*

6 – CONCLUSION

The off-axis compression and partial compression tests were conducted to investigate the spreading and damage zone effects

The failure mode was almost the same with or without the side margin. The kink band failure often occurred in the specimens at the loading angle of 0 degrees, and the stress-strain curves exhibited brittle behavior due to plastic buckling. The shear failure often occurred at 15 or 30 degrees, and the stress-strain curves exhibited brittle behavior. The compressive failure perpendicular to the grain often occurred at 30, 45, 60, and 90 degrees, and the stress-strain curves exhibited ductile behavior.

The proportional limit stress and Young's modulus almost increased with decreasing the loading angles. The proportional limit stress and Young's modulus of the specimens with the side margin are larger than those of the specimens without the side margin.

The spreading effect was present in most loading angles in the proportional limit stress and was present at loading angles of 45 degrees or more in the Young's modulus. The spreading effect increased as the loading angles increased.

The damage zone was present in all specimens with different loading angles, and the influence of the damage zone was particularly pronounced at the loading angles of 0 and 15 degrees.

Hankinson's equation with the exponent n=2 matches or slightly underestimates the average experimental values with or without side margin.

7 – REFERENCES

[1] H. Yoshihara, "Prediction of the off-axis stress-strain relation of wood under compression loading," *Eur. J. Wood Wood Prod.*, vol. 67, no. 2, pp. 183–188, 2009.

[2] J. Xavier, A. Majano-Majano, and J. Fernandez-Cabo, "Identifiability of stiffness components of clear wood from a single off-axes compression test," *Eur J Wood Wood Prod*, vol. 74, no. 3, pp. 285–290, 2016.

[3] N. T. Mascia and L. Vanalli, “Evaluation of the coefficients of mutual influence of wood through off-axis compression tests,” *Constr. Build. Mater.*, vol. 30, pp. 522–528, 2012.
[4] J. Garab, D. Keunecke, S. Hering, J. Szalai, and P. Niemz, “Measurement of standard and off-axis elastic moduli and Poisson’s ratios of spruce and yew wood in the transverse plane,” *Wood Sci. Technol.*, vol. 44, no. 3, pp. 451–464, 2010.
[5] S. C. Cowin, “On the strength anisotropy of bone and wood,” *J. Appl. Mech.*, vol. 46, no. 4, pp. 832–838, 1979.
[6] R. L. Hankinson, “Investigation of crushing strength of spruce at varying angles of grain,” *Air service information circular*, vol. 3, no. 259, 130, 1921.
[7] A. G. Zink, R. W. Davidson, and R. B. Hanna, “Strain Measurement in Wood using A Digital Image Correlation Technique,” *WFS*, pp. 346–359, 1995.
[8] M. Totsuka, R. Jockwer, H. Kawahara, K. Aoki, and M. Inayama, “Experimental study of compressive properties parallel to grain of glulam,” *J. Wood Sci.*, vol. 68, no. 1, 33, 2022.
[9] M. Totsuka, “Evaluation method of compression parallel to grain stiffness in wood and relationship between stiffness and shape of contact surface,” *Eur. J. Wood Wood Prod.*, vol. 83, no. 1, 15, 2025.
[10] D. Lathuilliere, O. Pop, L. Bléron, F. Dubois, F. Fouchal, and J.-F. Bocquet, “Spreading of transverse compressive stresses in glued laminated timber,” *Eur. J. Wood Wood Prod.*, vol. 73, no. 4, pp. 475–484, 2015.
[11] M. Totsuka, R. Jockwer, K. Aoki, and M. Inayama, “Experimental study on partial compression parallel to grain of solid timber,” *J. Wood Sci.*, vol. 67, no. 1, 39, 2021.
[12] JAS "Japanese Agricultural Standards for Gululam" Japanese Agricultural Standards, 2012.
[13] ASTM_D143-14 "Standard Test Methods for Small Clear Specimens of Timber".

https://doi.org/10.52202/080513-0673